

**Dynamics of liquid and undercooled silicon: An *ab initio* molecular dynamics study**N. Jakse<sup>1</sup> and A. Pasturel<sup>1,2</sup><sup>1</sup>*Sciences et Ingénierie des Matériaux et Procédés, INP Grenoble, UJF-CNRS 1130, rue de la Piscine, BP 75, 38402 Saint-Martin d'Hères Cedex, France*<sup>2</sup>*Laboratoire de Physique et Modélisation des Milieux Condensés, Maison des Magistères, BP 166 CNRS, 38042 Grenoble Cedex 09, France*

(Received 13 November 2008; published 27 April 2009)

First-principles molecular dynamics simulations of liquid and undercooled silicon have been performed in order to study the evolution of dynamic properties across the melting point. The calculated dynamic structure factors show collective excitations at small wave vectors above the melting point, in good agreement with recent experimental data, while the transverse current correlation functions do not display propagating shear modes. Upon undercooling, our results evidence the occurrence of well-defined shear modes that result from an enhancement of local tetrahedral arrangement associated to strong covalent bonding suggesting that propagating shear waves might be sustained by a concerted motion of tetrahedra.

DOI: [10.1103/PhysRevB.79.144206](https://doi.org/10.1103/PhysRevB.79.144206)

PACS number(s): 61.20.Lc, 61.20.Ja

**I. INTRODUCTION**

Silicon remains a seminal material which still plays an important role in semiconductor technology<sup>1</sup> and material design.<sup>2</sup> It also attracts growing interest in the context of energetic and environmental issues and specifically for the manufacturing of photovoltaic cells.<sup>3</sup> As crystalline silicon is usually generated from the melt, the knowledge of its properties in the liquid and undercooled states is then of considerable interest. In addition, the physical properties of liquid silicon displays many unusual aspects that have stimulated many experimental and theoretical researches, for instance a melting with a significant change in the local structure accompanied with a semiconductor-to-metal transition and, in the undercooled region, a quadratic behavior of the density as a function of temperature<sup>4</sup> as well as a liquid-liquid transition near  $T=1050$  K (Refs. 5 and 6) accompanied by an enhancement of the local tetrahedral structure.

The high melting temperature of silicon and its corrosive nature have hindered the experimental determination of its physical properties such as density,<sup>4</sup> diffusion,<sup>7</sup> and viscosity,<sup>4,8</sup> which have been measured accurately only recently. This is all the more true for the dynamic structure since the high velocity of sound (about 4000 m/s) represents an impediment for the use of inelastic neutron scattering. Recently, the dynamic structure factor  $S(q, \omega)$  has nevertheless been investigated by using a high-resolution inelastic x-ray scattering (IXS) technique<sup>9</sup> in order to cope with the question about the existence of collective excitations in liquid silicon as in other liquid metals.<sup>10</sup> It has been shown<sup>9</sup> that these excitations persist for wave vectors up to about half the position of the main peak of the static structure factor and are associated with the existence of a positive dispersion.

From a theoretical point of view, molecular dynamics (MD) simulations represent a powerful means to deal with the dynamic properties in the liquid state. They are able to give complementary information with respect to experiments and a comprehensive description about the single-atom as well as the collective behavior provided that atomic interactions are modeled accurately. In the only theoretical contri-

bution based on orbital-free MD simulations<sup>11</sup> of the longitudinal and transverse collective dynamics of liquid silicon, neither the positive dispersion in the longitudinal dispersion curve seen experimentally<sup>9</sup> nor transverse propagating modes have been found. This phenomenon has therefore to be reanalyzed since (i) transverse modes are not accessible to the experiment, and (ii) it is well known that the dynamics, and especially the collective dynamics, is very sensitive to the details of the interactions, and the use of orbital-free approximation could yield discrepancies with respect to the experiments. In this context, the use of first-principles-based simulations within the density-functional theory (DFT) is of primary importance, and up to now, for liquid silicon,<sup>12</sup> these simulations focused essentially to the static properties since the heaviness of the DFT calculations have restricted at that time the simulations to small numbers of atoms and too short time span to deal with the collective dynamic properties.

In the present paper, *ab initio* molecular dynamics (AIMD) simulations of liquid silicon have been performed using sufficiently large simulation box, namely, 512 atoms, over long times, i.e., 45 ps, to deal accurately with the collective dynamic properties. The calculated dynamic structure factors  $S(q, \omega)$  show collective excitations corresponding to propagating modes at small wave vectors in the liquid state above the melting point, in good agreement with the recent experimental findings.<sup>9</sup> Moreover, this allows us to deal with the important question of the evolution of the dynamic properties across the melting point from the liquid state above the melting point down to the deep undercooled regime in connection with our preceding work.<sup>6</sup> In order to provide a deeper insight into the dynamics mechanisms in the liquid and undercooled states, we have calculated the transverse current correlation functions. The latter give access to information about propagating shear modes that cannot be measured. Their presence in the liquid can be interpreted in terms of a viscoelastic behavior which is intermediate between a low-density system, which is not able to sustain these modes and a purely elastic solid in which they are proportional to the strain imposed.<sup>13</sup> Our results show that liquid Si does not display propagating shear modes above the melting point, in contrast to other liquid metals,<sup>10</sup> while they appear in the

deep undercooled regime. We discuss such a finding in terms of the structural evolution of liquid Si upon undercooling.

## II. SIMULATION METHOD

Investigations of the liquid and undercooled states have been performed using AIMD simulations with  $N=512$  silicon atoms within the DFT with the generalized gradient approximation (GGA).<sup>14</sup> We use the most recent version of the Vienna *ab initio* simulation package (VASP),<sup>15</sup> in which the interaction between the ions and electrons is described by the projector augmented-wave (PAW) method, as implemented by Kresse and Joubert.<sup>16</sup> In the PAW potential,  $2s$  and  $2p$  orbitals are treated as valence orbitals with a plane-wave cutoff of 245 eV and only the  $\Gamma$  point is used to sample the Brillouin zone. Molecular dynamics simulations were carried out with the Verlet algorithm in the velocity form with a time step of 1.5 fs and the phase-space trajectory was produced in the  $NVT$  (canonical) ensemble by means of a Nosé thermostat to control the temperature  $T$ . It is worth mentioning that Alfe and Gillan<sup>17</sup> determined the melting temperature of simulated silicon from first principles within the GGA using VASP. They have found a value  $T=1492 \pm 50$  K which is a bit lower than the experimental value of 1687 K. The use of PAW potentials here instead of ultrasoft pseudopotentials (USPP)<sup>16,18</sup> might induce only a very small difference in the melting temperature. Former first-principles calculations, carried out within the local-density approximation (LDA), yield a melting temperature of  $T=1350 \pm 10$  K,<sup>19</sup> indicating that the GGA is a better approximation as pointed out also by Alfe and Gillan.<sup>17</sup>

The simulation in the liquid state was performed at a temperature  $T=1750$  K, above the simulated and experimental melting temperatures, and with density  $\rho=0.055 \text{ \AA}^{-3}$  corresponding to the recent experimental value.<sup>4</sup> In the undercooled regime, the AIMD was performed in a thermodynamic state corresponding to a temperature  $T=1050$  K, which is below the simulated melting temperature, with a density  $\rho=0.0523 \text{ \AA}^{-3}$ ,<sup>6</sup> which is expanded with respect to the liquid state at 1750 K. We mention that the undercooled state was obtained from the combined classical and the first-principle MD simulations, as described in Ref. 5 and corresponds to the high density side of the liquid-liquid transition, below the density maximum. While such a density maximum in the undercooled region has not been observed yet experimentally, *ab initio* MD simulations reported recently yield a maximum at about 1200 K.<sup>20</sup> It is well known that the Stillinger-Weber empirical potential exhibit also a density maximum<sup>5,6,21</sup> but underestimates the experimental density<sup>4</sup> at the melting point. In the simulations, the system was equilibrated during 10 ps and calculations of dynamic properties were done during a time span of 45 ps at  $T=1750$  K and 70 ps at  $T=1050$  K. The calculated pressures are 1.89 GPa at  $T=1750$  K and 1.34 GPa at  $T=1050$  K. The pressure difference cannot be considered as negligible however it lies within the fluctuations, which are of the order of 1.2 GPa. On the other hand, the temperature fluctuations are relatively small, namely, 100 K at  $T=1750$  K and 75 K at  $T=1050$  K. Consequently, given the melting temperatures of

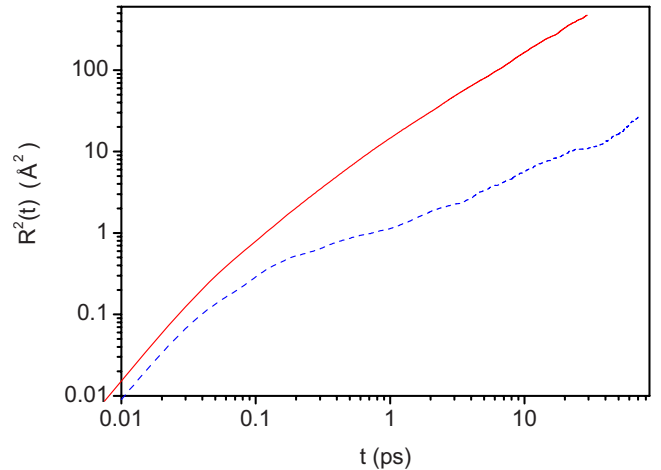


FIG. 1. (Color online) Mean-square displacement calculated from the AIMD simulations in the liquid state (solid line) and in the undercooled region (dashed line).

simulated silicon mentioned above,<sup>17,19</sup> the two states are unambiguously in the stable and undercooled regimes, respectively.

## III. RESULTS AND DISCUSSION

### A. Single-particle dynamics: Diffusion

In order to check that the system remains liquid, especially in the deep undercooled regime at  $T=1050$  K, we have determined the self-diffusion coefficient  $D$  from the slope of the mean-square displacement,

$$\langle R^2(t) \rangle = \frac{1}{N} \left\langle \sum_{i=1}^N [\mathbf{r}_i(t) - \mathbf{r}_i(t=0)]^2 \right\rangle, \quad (1)$$

where  $\mathbf{r}_i(t)$  denotes the position of atom  $i$  at time  $t$ . Figure 1 shows the behavior of  $R^2(t)$  as a function of time in the logarithmic scale for both temperatures. While in the liquid state the ballistic regime below 0.1 ps is followed directly by a fast diffusive regime, in the undercooled state, the system displays a marked cage effect which lasts nearly 5 ps before entering the diffusion characteristic of a liquid.

From the linear slope of  $R^2(t)$  at large  $t$ , we have obtained  $D=2.73 \text{ \AA}^2/\text{ps}$  at  $T=1750$  K which is compatible with the experimental value  $D=2.52 \text{ \AA}^2/\text{ps}$  inferred from surface tension measurements<sup>6</sup> at the melting temperature ( $T_m=1687$  K). It is worth mentioning that previous *ab initio* molecular dynamics simulations of Stich *et al.* and Godlevsky *et al.*<sup>12</sup> for liquid Si, yield values of  $D$  between  $1.9 \text{ \AA}^2/\text{ps}$  with 64 atoms within the LDA and  $3.1 \text{ \AA}^2/\text{ps}$  with 350 atoms using a spin-dependent treatment for the electrons in the framework of the GGA. The orbital-free AIMD simulation with 2000 atoms<sup>11</sup> leads to  $D=2.28 \text{ \AA}^2/\text{ps}$ . Other MD simulations using empirical and tight-binding potentials have also been performed to estimate the self-diffusion coefficient,<sup>21,22</sup> but much lower values are obtained. In the general case these potentials overestimate the covalent bonding for this element that could explain this feature. In the undercooled state at  $T=1050$  K the system

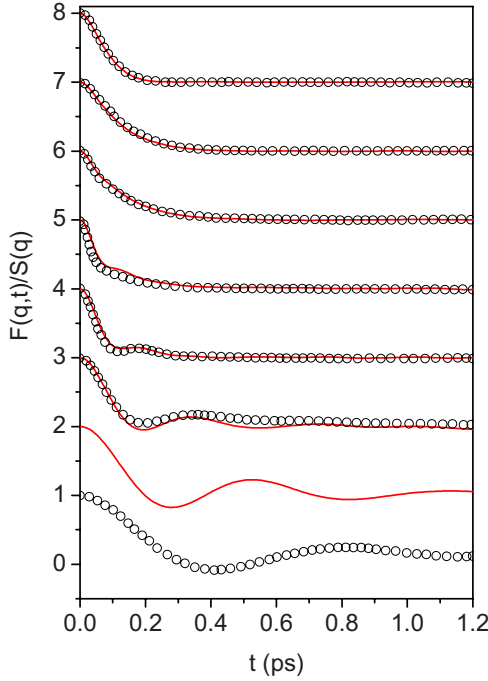


FIG. 2. (Color online) Intermediate scattering function calculated from the AIMD simulations in the liquid state (solid lines) for several  $q$ -values. The curves for  $q=0.29, 0.42, 0.72, 1.10, 1.89, 2.50,$  and  $2.89 \text{ \AA}^{-1}$  from the bottom to the top are shifted upward by an amount of 1, 2, 3, 4, 5, 6, and 7, respectively. The open circles correspond to the experimental data of Ref. 8 for  $q=0.20, 0.43, 0.74, 1.12, 1.89, 2.50,$  and  $2.89 \text{ \AA}^{-1}$  from the bottom to the top.

still diffuses and we have found  $D=0.062 \text{ \AA}^2/\text{ps}$ , which is more than 40 times lower than in the stable liquid.

## B. Collective dynamics

### 1. Dynamic structure factor and longitudinal current correlation function

Information about the collective dynamics is obtained through the intermediate scattering function

$$F(q,t) = \frac{1}{N} \left\langle \sum_{k,l=1}^N \exp\{i\mathbf{q}[\mathbf{r}_k(t) - \mathbf{r}_l(t=0)]\} \right\rangle, \quad (2)$$

where  $\mathbf{q}=(2\pi/L)(n_x, n_y, n_z)$  are wave vectors compatible with the length  $L=V^{1/3}$  of the cubic simulation cell and numbers  $n_x, n_y,$  and  $n_z$  are integers. Function  $F(q,t)$  is of general interest since its time Fourier transform is the dynamic structure factor  $S(q,\omega)$  directly measurable from inelastic scattering experiments.

For liquid silicon close to melting, namely,  $T=1733 \text{ K}$ , Hosokawa *et al.*<sup>9</sup> succeeded recently in performing IXS measurements of  $S(q,\omega)$ , and the quality of their data allows for the determination of the intermediate scattering function  $F(q,t)$ . In Fig. 2, the results of  $F(q,t)$  from our AIMD simulations at  $T=1750 \text{ K}$  are compared with the experimental data as a function of time for the selected  $q$  values. As  $q$  decreases the behavior of the intermediate scattering function changes from an exponential decay to a damped oscillatory

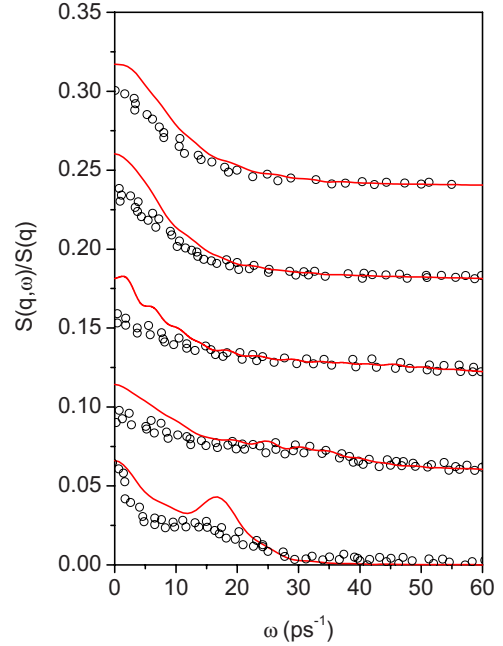


FIG. 3. (Color online) Dynamic structure factor calculated from the AIMD simulations in the liquid state (solid lines) for several  $q$ -values. The curves for  $q=0.42, 0.72, 1.10, 1.89,$  and  $2.50 \text{ \AA}^{-1}$  from the bottom to the top are shifted upward by an amount of 0, 0.06, 0.12, 0.18, and 0.24, respectively. The open circles correspond to the experimental data of Ref. 8 for  $q=0.43, 0.74, 1.12, 1.89,$  and  $2.50 \text{ \AA}^{-1}$  from the bottom to the top.

regime at about  $q=1.10 \text{ \AA}^{-1}$ , in agreement with experiments. The presence of these oscillations is a clear signature of collective excitations in the liquid. Due to the size of the simulation cell, the lowest  $q$  value that can be reached for the determination of  $F(q,t)$  is  $q=0.29 \text{ \AA}^{-1}$ , nevertheless the calculated curve is in line with the measurements that were done down to  $q=0.20 \text{ \AA}^{-1}$ . It is worth mentioning that below  $q=1.10 \text{ \AA}^{-1}$ ,  $F(q,t)$  has a Gaussian behavior at short time and a small thermal diffusive component in the oscillations which can be modeled in the framework of the hydrodynamic theory<sup>10</sup> as an exponential decay.

Figure 3 displays the AIMD dynamic structure factors  $S(q,\omega)$  compared to the corresponding experimental data<sup>9</sup> for several  $q$  values. Although the calculated curves underestimate the central peak with respect to experiments, the position in frequency of the inelastic peak occurring for  $q$  values below  $1.10 \text{ \AA}^{-1}$ , as well as its increase with increasing  $q$  is nicely reproduced. This shows that propagating collective excitations, which are present in liquid Si, are well described by our AIMD simulations.

The collective excitations seen on the dynamic structure factor are also present in the corresponding longitudinal current-current correlation function  $C_L(q,\omega)=\omega^2 S(q,\omega)/q^2$  and correspond to the position of its single maximum of frequency  $\omega_L$ . The dispersion curve is then constructed from the positions of the maximum of  $C_L(q,\omega)$  for each value of  $q$  where a side peak is detected. The resulting curve shown in Fig. 4 is in good agreement with the experimental one.<sup>9</sup> We have inferred the value of  $c_L=3800 \text{ m s}^{-1}$  by a linear fitting of the simulation data for the two smallest values of  $q$ . Our

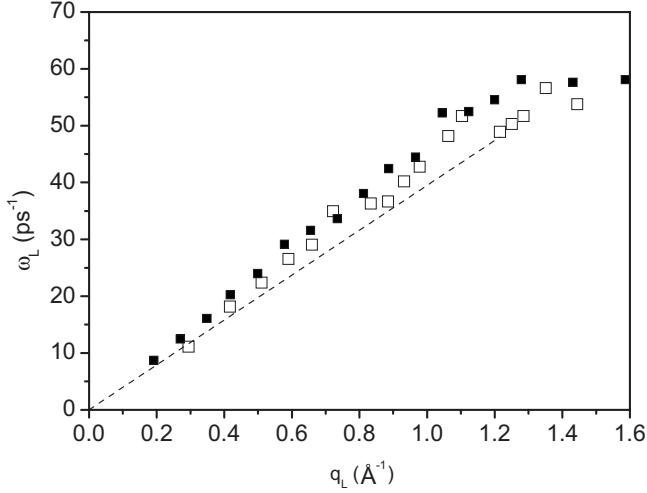


FIG. 4. Longitudinal dispersion curve calculated from the AIMD in the liquid state (open squares) compared to the experimental data of Ref. 8 (full squares). The dashed lines correspond to a linear fit of the simulated curve at small  $q$  (see text).

result gives a prediction of the sound velocity which is in fair agreement with the experimental values of the adiabatic sound velocity, namely,  $3952 \text{ m s}^{-1}$  at  $T=1733 \text{ K}$  (Ref. 9) and  $3977 \text{ m s}^{-1}$  at  $T=1753 \text{ K}$ .<sup>23</sup> Hosokawa *et al.*<sup>9</sup> reported that the frequencies  $\omega_L(q)$  display a positive dispersion, i.e., increase faster than the hydrodynamic linear dispersion. Concerning our results such a positive dispersion seems to occur however this effect is small and we will refrain from firmly establishing that such a positive dispersion takes place in our simulations. Upon undercooling, the dynamic structure factor (not shown) displays also collective modes that occur at higher frequencies than in the stable liquid.<sup>6</sup> As a result, the dispersion curve obtained from the corresponding longitudinal current correlation functions gives rise to a sound velocity of  $6960 \text{ m s}^{-1}$  which is nearly twice higher than the value above the melting point.

## 2. Transverse current correlation function

We consider now the transverse current correlation function

$$C_T(q, t) = \frac{1}{N} \langle J_T^*(q, t) J_T(q, t) \rangle, \quad (3)$$

which is defined in terms of  $J_T(q, t)$ , the transverse current written along the  $x$  direction as

$$J_T(q, t) = \sum_{j=1}^N v_{j,x}(t) \exp[iqz_j(t)], \quad (4)$$

where  $v_{i,x}(t)$  is the  $x$  component of the velocity of atom  $i$  and  $q$  is a wave vector along the  $z$  direction. Two formally identical expressions can be written for  $y$  and  $z$  directions. It is worth noticing that this function is not experimentally accessible, but it is of fundamental interest since it gives access to the calculation of the shear viscosity and to the analysis of the propagating shear modes. As a matter of fact, its zero-

limit Laplace transform  $\tilde{C}_T(q, z=0)$  leads to the  $q$ -dependent shear viscosity

$$\eta(q) = \frac{\rho k_B T}{mq^2 \tilde{C}_T(q, z=0)}. \quad (5)$$

where  $m$  stands for the average mass of the atoms and  $\rho$  is the number density. The shear viscosity  $\eta$  can be inferred by extrapolating  $\eta(q)$  to  $q=0$ .<sup>24</sup> Using a fitting function  $\eta(q) = \eta / (1 + a^2 q^2)$  (Ref. 25) we have obtained  $\eta=0.064 \text{ mPa s}$  at  $T=1750 \text{ K}$ , in close agreement with the recent experimental value  $\eta=0.052 \text{ mPa s}$  (Ref. 4) and also in the range of preceding experimental results.<sup>8</sup> Due to the very slow diffusion in the undercooled state, it was not possible within this formalism to calculate the shear viscosity, which is presumably very high.

The Fourier transform of  $C_T(q, t)$  yields the spectral function  $C_T(q, \omega)$  which can display a well-defined peak at non-zero frequencies for sufficiently dense liquids.<sup>26</sup> The position of this so-called inelastic peak, appearing in a specific  $q$

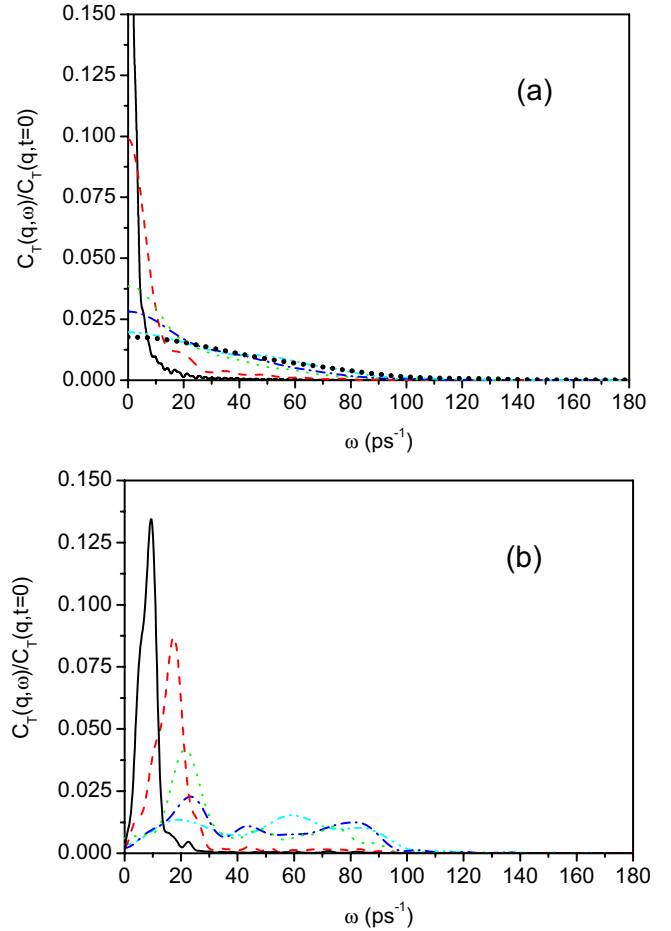


FIG. 5. (Color online) Transverse current correlation functions calculated from the AIMD (a) in the liquid state for  $q=0.29$  (solid line),  $0.58$  (dashed line),  $1.17$  (dotted line),  $1.47$  (dot-dashed line),  $2.06$  (dot-dot-dashed line),  $3.53 \text{ \AA}^{-1}$  (large dots), and (b) in the undercooled region for  $q=0.29$  (solid line),  $0.58$  (dashed line),  $1.17$  (dotted line),  $1.47$  (dot-dashed line), and  $2.06 \text{ \AA}^{-1}$  (dot-dot-dashed line).

range, corresponds to propagating shear modes that are usually attributed to viscoelastic effects. In Fig. 5(a), the function  $C_T(q, \omega)$  is drawn for selected  $q$  values for  $T=1750$  K above the melting point and  $T=1050$  K in the undercooled regime. At  $T=1750$  K,  $C_T(q, \omega)$  displays an elastic peak at  $\omega=0$  which behaves rather as a Lorentzian at low  $q$  (hydrodynamic regime) and as a Gaussian at larger  $q$  (kinetic regime).<sup>10</sup> For all the  $q$  values,  $C_T(q, \omega)$  displays a monotonic decrease indicating that no propagating shear modes are present in liquid Si. This feature was also observed by Delisle *et al.*<sup>11</sup> from their orbital-free AIMD for liquid Si. Upon undercooling, as can be seen on Fig. 5(b), the functions  $C_T(q, \omega)$  exhibit a marked inelastic peak for all  $q$  values compatible with the size of the simulation cell below  $1.18 \text{ \AA}^{-1}$ . At larger  $q$ , the peak of  $C_T(q, \omega)$  tends to disappear in a background spreading up to  $\omega=100 \text{ ps}^{-1}$ . The frequency of the peak maximum increases with increasing  $q$ , indicating clearly propagating modes roughly up to  $\omega=25 \text{ ps}^{-1}$  and giving rise to the dispersion curve associated with a transverse sound velocity  $c_T=3220 \text{ m s}^{-1}$ .<sup>6</sup>

The fact that the spectra of the transverse current correlation functions do not display an inelastic peak, reflecting therefore the absence of propagating shear waves, is in contrast with what is found usually for dense liquid metals near the melting point (See Ref. 9 and references therein). Such a situation for liquid Si can be understood by the fact that generally low-density and high-temperature liquids cannot sustain shear waves, and is supported by a high diffusivity and an absence of cage effect, as can be seen on Fig. 1. When liquid Si is deeply undercooled, the functions  $C_T(q, \omega)$  displaying a marked inelastic peak show propagating shear waves. Since the densities in the liquid and the undercooled states are not very different (they differ less than 5%), their appearance might not be attributed to density effects. As shown in our previous works,<sup>6</sup> the undercooling of liquid Si induces an increase of the local tetrahedral arrangement re-

vealing the increase of the covalent bonding in the system. As pointed out by Canales and Padro,<sup>26</sup> the enhancement of attractive interatomic forces favors significantly the propagation of shear modes. Therefore our results strongly suggest that the appearance of shear waves might be due the enhancement of local tetrahedral arrangements associated to strong covalent bonding and that the propagating shear waves might be sustained by a concerted motion of tetrahedra.

#### IV. CONCLUSION

In the present work, AIMD simulations of liquid silicon have been performed in order to study the evolution of the dynamic properties of silicon across the melting point, from the liquid state above the melting point down to the deep undercooled regime. In the liquid state above the melting point, the calculated dynamic structure factors  $S(q, \omega)$  show collective excitations at small wave vectors, in good agreement with the recent experimental data, while by inspecting the transverse current correlation functions no propagating shear modes are present. Well defined shear modes appear in the deep undercooled regime, which result from an enhancement of local tetrahedral arrangement associated to strong covalent bonding. Our findings strongly suggest that the propagating shear waves might be sustained by a concerted motion of tetrahedra and shed some light upon structure-dynamics correlations.

#### ACKNOWLEDGMENTS

We acknowledge the CINES and IDRIS under Project No. INP2227/72914 as well as PHYNUM CIMENT for computational resources. The ANR is gratefully acknowledged for financial support under Grant No. ANR:BLAN06-3\_138079.

<sup>1</sup>W. C. O'Mara, R. B. Herring, and L. P. Hunt, *Handbook of Semiconductor Silicon Technology* (William Andrew Publishing/Noyes, Norwich, NY, 1990).

<sup>2</sup>A. Inoue, *Acta Mater.* **48**, 279 (2000).

<sup>3</sup>A. Müller, M. Ghosh, R. Sonnenschein, and P. Woditsch, *Mater. Sci. Eng., B* **134**, 257 (2006).

<sup>4</sup>Z. Zhou, S. Mukherjee, and W. K. Rhim, *J. Cryst. Growth* **257**, 350 (2003).

<sup>5</sup>S. Sastry and C. A. Angell, *Nature Mater.* **2**, 739 (2003); S. S. Ashwin, U. V. Waghmare, and S. Sastry, *Phys. Rev. Lett.* **92**, 175701 (2004).

<sup>6</sup>N. Jakse and A. Pasturel, *Phys. Rev. Lett.* **99**, 205702 (2007); N. Jakse and A. Pasturel, *J. Chem. Phys.* **129**, 104503 (2008).

<sup>7</sup>H. M. Lu, T. H. Wang, and Q. Jiang, *J. Cryst. Growth* **293**, 294 (2006).

<sup>8</sup>H. Sasaki, E. Tokizaki, X. M. Huang, K. Terashima, and S. Kimura, *Jpn. J. Appl. Phys., Suppl.* **34**, 3432 (1995); S. Kimura and K. Terashima, *J. Cryst. Growth* **180**, 323 (1997).

<sup>9</sup>S. Hosokawa, W.-C. Pilgrim, Y. Kawakita, K. Ohshima, S. Takeda, D. Ishikawa, S. Tsutsui, Y. Tanaka, and A. Q. R. Baron,

*J. Phys.: Condens. Matter* **15**, L623 (2003); S. Hosokawa, J. Greif, F. Demmel, and W.-C. Pilgrim, *Nucl. Instrum. Methods Phys. Res. B* **199**, 161 (2003).

<sup>10</sup>T. Scopigno, G. Ruocco, and F. Sette, *Rev. Mod. Phys.* **77**, 881 (2005).

<sup>11</sup>A. Delisle, D. J. González, and M. J. Stott, *Phys. Rev. B* **73**, 064202 (2006).

<sup>12</sup>I. Stich, R. Car, and M. Parrinello, *Phys. Rev. Lett.* **63**, 2240 (1989); *Phys. Rev. B* **44**, 4262 (1991); I. Stich, *Phys. Rev. A* **44**, 1401 (1991); I. Stich, M. Parrinello, and J. M. Holender, *Phys. Rev. Lett.* **76**, 2077 (1996); V. Godlevsky, J. R. Chelikowsky, and N. Troullier, *Phys. Rev. B* **52**, 13281 (1995).

<sup>13</sup>S. P. Das, *Rev. Mod. Phys.* **76**, 785 (2004).

<sup>14</sup>Y. Wang and J. P. Perdew, *Phys. Rev. B* **44**, 13298 (1991).

<sup>15</sup>G. Kresse and J. Furthmüller, *Comput. Mater. Sci.* **6**, 15 (1996); *Phys. Rev. B* **54**, 11169 (1996).

<sup>16</sup>G. Kresse and D. Joubert, *Phys. Rev. B* **59**, 1758 (1999).

<sup>17</sup>D. Alfe and M. J. Gillan, *Phys. Rev. B* **68**, 205212 (2003).

<sup>18</sup>D. Vanderbilt, *Phys. Rev. B* **41**, 7892 (1990).

<sup>19</sup>O. Sugino and R. Car, *Phys. Rev. Lett.* **74**, 1823 (1995).

- <sup>20</sup>G. J. Ackland, Phys. Rev. Lett. **97**, 015502 (2006).
- <sup>21</sup>J. Q. Broughton and X. P. Li, Phys. Rev. B **35**, 9120 (1987).
- <sup>22</sup>C. Z. Wang, C. T. Chan, and K. M. Ho, Phys. Rev. Lett. **66**, 189 (1991); Phys. Rev. B **45**, 12227 (1992); R. Virkkunen, K. Laasonen, and R. M. Nieminen, J. Phys.: Condens. Matter **3**, 7455 (1991); W. Yu, Z. Q. Wang, and D. Stroud, Phys. Rev. B **54**, 13946 (1996); N. Jakse, Y. Kadiri, and J. L. Bretonnet, *ibid.* **61**, 14287 (2000); Y. Kadiri, N. Jakse, and J. L. Bretonnet, J. Non-Cryst. Solids **312-314**, 143 (2002).
- <sup>23</sup>N. Yoshimoto, M. Ikeda, M. Yoshizawa, and S. Kimura, Physica B **219-220**, 623 (1996).
- <sup>24</sup>N. Jakse, J. F. Wax, and A. Pasturel, J. Chem. Phys. **126**, 234508 (2007).
- <sup>25</sup>W. E. Alley and B. J. Alder, Phys. Rev. A **27**, 3158 (1983).
- <sup>26</sup>M. Canales and J. A. Padro, Phys. Rev. E **60**, 551 (1999).